Streptolysin O derived from *Streptococcus pyogenes* inhibits RANKL-induced osteoclastogenesis through the NF-κB signaling pathway

JIN YI[1], RUOHUI TANG[1], JING YANG[1], YUEQI CHEN[2] and JUN FEI[1,3]

[1]Centre of Trauma of PLA, Daping Hospital, Third Military Medical University, Chongqing 400042;
[2]Department of Biomedical Materials Science, School of Biomedical Engineering; [3]State Key Laboratory of Trauma, Burn and Combined Injury, Third Military Medical University, Chongqing 400038, P.R. China

Abstract. *Streptococcus pyogenes* (GAS) is a clinically significant bacterial strain that causes bacterial arthritis, osteomyelitis and implant infections. Infection complications can lead to serious bone destruction. Osteoclasts, the only type of cell with bone resorption function, participate in this process. Streptolysin O (SLO) is produced by almost all clinical *Streptococcus pyogenes* isolates. However, the role of SLO in bone infection caused by GAS had not been previously examined. The current study was performed to define the effects of SLO on receptor activator of NF-κB ligand-stimulated osteoclast differentiation *in vitro*. Results demonstrated that SLO decreased the phosphorylation of p65 and NF-κB inhibitor α, suppressed c-FOS and nuclear factor of activated T-cells cytoplasmic 1, and downregulated the expression of osteoclast marker genes. SLO also induced apoptosis of mature osteoclasts. The results suggested that SLO blocked osteoclast activation during GAS infection. These findings may prove useful in the development of novel strategies for treating GAS-associated bone infectious diseases.

Correspondence to: Professor Jun Fei, Centre of Trauma of PLA, Daping Hospital, Third Military Medical University, 10 Changjiang Zhilu, Chongqing 400042, P.R. China
E-mail: feijundoctor@sohu.com

Abbreviations: M-CSF, macrophage colony-stimulating factor; NFATc1, nuclear factor of activated T cells cytoplasmic 1; NF-κB, nuclear factor-κB; RANKL, receptor activator of NF-κB ligand; TRAP, tartrate-resistant acid phosphatase; GAS, *streptococcus pyogenes*; SLO, streptolysin O; CTR, calcitonin receptor; ATP6v0d2, ATPase H+ transporting V0 subunit d2; DC-STAMP, dendritic cell-specific transmembrane protein; MMP9, matrix metalloproteinase-9; PGN, peptidoglycan

Introduction

Bone is a dynamic organ undergoing continual remodeling to grow, repair damage, and regulate calcium and phosphate metabolism in the body. The bone remodeling process is tightly regulated, controlling bone resorption by osteoclasts and bone formation by osteoblasts (1). Osteoclasts are the sole cell-type with bone resorption function. Abnormal activation of osteoclasts during bone infections, including bacterial sepsis, osteomyelitis and implant infections, can cause pathological bone destruction, resulting in bone non-union and delayed fracture healing (2).

Bone infection is a serious complication in orthopedics, and the rate of infection associated with open fractures is 3-40% (3). *Streptococcus pyogenes* (GAS) is among the most important bacterial strains that cause bone infections, including septic arthritis and osteomyelitis, and is involved in the inflammatory destruction of joints and bones. GAS accounts for ~15% of all cases of nongonococcal bacterial arthritis, which causes serious morbidities (4). Antibiotics and debridements are a burden on medical resources as they are time-consuming and expensive. Although penicillin is effective against the majority of GAS strains, 20-40% of cases occur during treatment with antibiotics (5). GAS bone infections are likely to be a continuing and increasing problem, and an improved understanding of the interaction between GAS and bone is essential for the development of novel therapeutic strategies for treating antibiotic-resistant and persistent infections.

Streptolysin O (SLO) is well characterized and considered to be an important virulence factor produced by the majority of clinical GAS isolates, and overexpressed in invasive infections (6). SLO is a cholesterol-dependent cytolysin (CDC), a large family of toxins produced by the majority of ram-positive bacterial strains, of which many have been characterized as important virulence factors. CDCs bind to cholesterol-containing membranes where they oligomerize and insert into the lipid bilayer to form large pores (7-9). SLO can deliver exogenous molecules to the cytoplasm, including other toxins produced by GAS through the pores (10). Furthermore, SLO can interact with a number of cell types, including polymorphonuclear neutrophils, macrophages and keratinocytes. In keratinocytes, SLO is associated with enhanced intracellular survival of

GAS (11). GAS resistance to macrophages primarily depends on the pore-forming toxin, SLO (12). However, the exact role of SLO in bone destruction induced by GAS remains unknown.

Therefore, the present study aimed to determine whether SLO is involved in GAS-induced bone destruction. Herein, it was demonstrated that SLO was able to suppressing receptor activator of NF-κB ligand (RANKL)-induced osteoclast differentiation and promoting mature osteoclast apoptosis. These results may help discover novel strategies to be applied following failed treatment of bone infections caused by GAS.

Materials and methods

Reagents and chemicals. Dulbecco's modified Eagle's medium (DMEM) and fetal bovine serum (FBS) were obtained from Gibco (Thermo Fisher Scientific, Inc., Waltham, MA, USA). The Cell Counting kit-8 (CCK-8) was purchased from Dojindo Molecular Technologies, Inc. (Kumamoto, Japan). Recombinant mouse macrophage colony-stimulating factor (M-CSF) and recombinant mouse RANKL were purchased from R&D Systems, Inc. (Minneapolis, MN, USA). The Osteo assay surface 96-well plates were obtained from Corning Incorporated (Corning, NY, USA). SLO was obtained from Beijing Ambition Biotechnology, Co., Ltd. (Beijing, China). The tartrate-resistant acid phosphatase (TRAP) stain kit was obtained from Sigma-Aldrich (Merck KGaA). Actin cytoskeleton and focal adhesion staining kits were purchased from EMD Millipore (Billerica, MA, USA). Specific primary antibodies against NF-κB inhibitor α (IκBα; cat. no. BS3601), phosphor (p)-IκBα (cat. no. BS4105), p65 (cat. no. BS3648), p-p65 (cat. no. BS4140), BCL2 associated X, apoptosis regulator (Bax; cat. no. BS1030), BCL2, apoptosis regulator (Bcl-2; cat. no. BS70205), caspase-3 (cat. no. BS9872 M), Fos proto-onco-gene (c-FOS; cat. no. BS6433), nuclear factor of activated T cells 1 (NFATc1; cat. no. BS6677), GAPDH (cat. no. AP0063) and secondary antibody (cat. no. BS13271) were obtained from Bioworld Technology, Inc. (St. Louis Park, MN, USA). Raw 264.7 cells were purchased from the American Type Culture Collection (Manassas, VA, USA).

Cell viability assays. Raw 264.7 cells were seeded in 96-well plates at a density of $3x10^3$ cells/well. Following culture in DMEM containing 10% FBS for 10 h, the cells were incubated with different concentrations of SLO (0, 0.25, 0.5, 1, 2.5, 5 and 10 μg/ml) for 24 or 72 h. The cell medium and SLO were replaced every 2 days. A total of 10 μl CCK-8 buffer and 90 μl medium were added to each well prior to incubation at 37℃ for another 2 h. The absorbance was measured at 450 nm using a multi-detection microplate reader.

TRAP staining assay. Raw 264.7 cells were cultured with DMEM containing 10% FBS for 10 h in 96-well plates at a density of $3x10^3$ cells/well. Following incubation with 100 μl DMEM containing 50 ng/ml RANKL, 50 ng/ml M-CSF and different concentrations of SLO (0, 0.25, 0.5, 1 and 2.5 μg/ml) for 72 h, cells were washed twice with PBS. Then the cells were fixed with 4% paraformaldehyde at 37℃ for 5 min and stained with a TRAP staining solution (100 μl) at 37℃ for 3 h. Osteoclasts were identified by positive staining for TRAP. TRAP-positive cells with >3 nuclei were counted under a microscope (3 fields/wells).

Actin cytoskeleton and focal adhesion staining. To measure actin cytoskeleton and focal adhesion kinase staining, Raw 264.7 cells ($3x10^3$ cells/well) were incubated in 100 μl DMEM with 50 ng/ml RANKL and 50 ng/ml M-CSF, then fixed with 4% paraformaldehyde for 15 min at room temperature prior to permeabilization for 5 min with 0.1% Triton X-100 at 24℃. Following blocking with bovine serum albumin (BSA) (Beyotime Institute of Biotechnology, Shanghai, China), cells were incubated with primary antibody solution (cat. no. FAK 100; anti-vinculin, 1:500) for 1 h, then washed with BSA three times. Cells were incubated with **tetramethylrhoda-mine-conjugated phalloidin** diluted in PBS (1:300) for 50 min at room temperature. Finally, cells were incubated with DAPI (1:1,000) for 5 min at 24℃. Fluorescence was detected using a fluorescence microscope (3 fields/wells).

Bone resorption assay. To measure the bone resorption of osteoclasts, Raw 264.7 cells ($3x10^3$ cells/well) were seeded into Osteo assay surface 96-well plates (Corning Incorporated, Corning, NY, USA). The cells were cultured in 100 μl medium containing 50 ng/ml RANKL and 50 ng/ml M-CSF with different concentrations of SLO for 5 days. The medium was removed and washed with sodium hypochlorite once, followed by three washes with PBS. Following drying of the plates, bone resorption pits were detected by under a light microscope and analyzed with ImageJ software version 1.37V (National Institutes of Health, Bethesda, MD, USA; 3 fields/wells).

RNA extraction and reverse transcription-quantitative polymerase chain reaction (RT-qPCR). To measure specific gene expression during osteoclastogenesis, a total of $2.4x10^4$ Raw 264.7 cells were seeded per well in 12-well plates and cultured with 800 μl DMEM containing 50 ng/ml RANKL and 50 ng/ml M-CSF. Cells were incubated with SLO (0, 0.25, 0.5, 1 and 2.5 μg/ml) for 3 days until mature osteoclasts were identifiable using a light microscope. Total mRNA was extracted using TRIzol reagent. Genomic DNA was removed at 42℃ for 2 min. The cDNA was synthesized from 1 μg total RNA using reverse transcriptase with oligo-dT primers at 37℃ for 15 min followed by 85℃ for 5 sec, according the manufacturer's instructions (Takara Biotechnology Co., Ltd., Dalian, China), then subjected to PCR amplification (BGI-Tech Solutions Co., Ltd., Shenzhen, China). The PCR product was quantified by qPCR using SYBR-Green Mix with the ΔΔCq method (13). qPCR was performed with the following thermocycling conditions: Pre-incubation at 95℃ for 30 sec, followed by 40 cycles of amplification at 95℃ for 5 sec and 60℃ for 1 min, and then cooling at 65℃ for 5 sec. The primers for TRAP, calcitonin receptor (CTR), integrinβ3, ATPase H$^+$ transporting V0 subunit d2 (ATP6v0d2), dendritic cell-specific transmembrane protein (DC-STAMP), matrix metalloproteinase-9 (MMP9) and GAPDH are presented in Table I. GAPDH was used as an internal control.

Western blotting. A total of $3x10^4$ Raw 264.7 cells were seeded per well in 6-well plates and cultured with 1 ml DMEM containing 50 ng/ml RANKL, 50 ng/ml M-CSF varying concentrations of SLO. Raw 264.7 cells were collected from 6-well plates and lysed with **phenylmethane sulfonyl fluoride buffer and phospha-tase inhibitors** 3 days after mature osteoclasts were identified. Following centrifugation at 4,024.8 x g for 10 min at 4℃ to

Table I. Primer sequences for reverse transcription-quantitative polymerase chain reaction.

Primer	Forward (5'-3')	Reverse (5'-3')
TRAP	CACTCCCACCCTGAGATTTGT	CATCGTCTGCACGGTTCTG
CTR	CGCATCCGCTTGAATGTG	TCTGTCTTTCCCCAGGAAATGA
Integrin β	TGTGTGCCTGGTGCTCAGA	AGCAGGTTCTCCTTCAGGTTACA
ATP6v60d2	CAGAGCTGTACTTCAATGTGGAC	AGGTCTCACACTGCACTAGGT
DC-STAMP	CTAGCTGGCTGGACTTCATCC	TCATGCTGTCTAGGAGACCTC
MMP9	CTGGACAGCCAGACACTAAAG	CTCGCGGCAAGTCTTCAGAG
GAPDH	AAATGGTGAAGGTCGGTGTG	TGAAGGGGTCGTTGATGG

TRAP, tartrate-resistant acid phosphatase; CTR, calcitonin receptor; DC-STAMP, DC-STAMP, dendritic cell-specific transmembrane protein; MMP, matrix metalloproteinase.
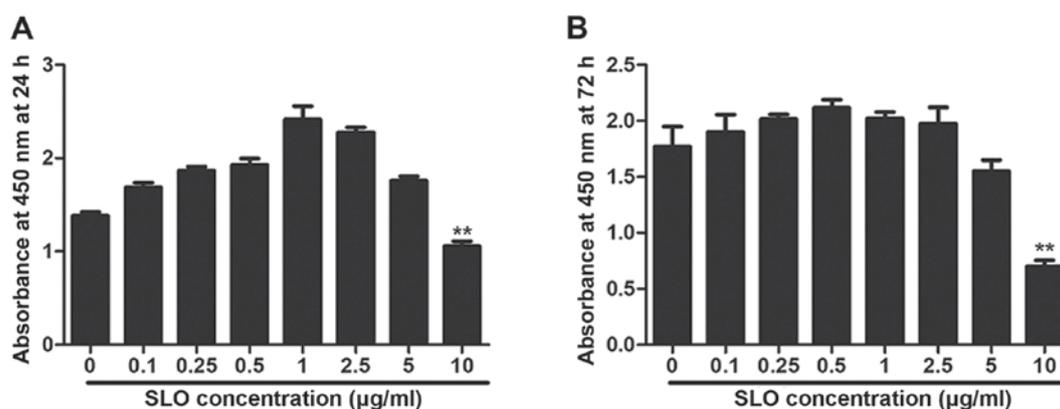

Figure 1. SLO toxicity evaluation *in vitro*. RAW 264.7 cells were cultured in medium containing 10% fetal bovine serum with the indicated dosages of SLO for (A) 24 h and (B) 72 h. Cell viability was measured by Cell Counting kit-8 assay. **$P<0.01$ vs. 0 μg/ml SLO. SLO, streptolysin O.

collect the supernatant, the protein concentration was determined by bicinchoninic acid assay. Equal volumes of protein samples were mixed with 5X sample loading buffer and heated at 95˚C for 10 min. Protein (40 μg) was loaded per lane. Following separation by 10% SDS-PAGE, protein was transferred to a polyvinylidene difluoride membrane. The membrane was blocked in 5% skimmed milk in TBS-Tween for 3 h at 24˚C, and incubated overnight at 4˚C with primary antibody (1:1,000) against IκBα, p-IκBα, p65, p-p65, Bax, Bcl-2, Caspase-3, c-FOS, NFATc1 and GAPDH. The blots were then washed in TBS-T three times, incubated for 1.5 h at room temperature with secondary antibody (1:1,000), and washed again prior to signal detection using BeyoECL Star (Beyotime Institute of Biotechnology). GAPDH was used as an internal control.

Cell apoptosis assay. Raw 264.7 cells (3x10⁴ cells/well) were collected from 6-well plates following culture 72 h. Following centrifugation at 1,006.2 x g for 4 min at 24˚C, the supernatant was removed and the cells were stained with Annexin-V-fluorescein isothiocyanate and propidium iodide for 15 min at 4˚C in the dark. The apoptotic rate was measured at 488 nm by flow cytometry and analyzed with FlowJo 10.0.7 (FlowJo LLC, Ashland, OR, USA).

Statistical analysis. SPSS 18.0 (SPSS, Inc., Chicago, IL, USA) was used for statistical analysis. The data are expressed as the mean ± standard deviation. Multiple groups were performed using one-way analysis of variance, with Bonferroni post hoc tests. $P<0.05$ was considered to indicate a statistically significant difference.

Results

SLO toxicity evaluation. The toxicity of SLO was measured in a CCK-8 assay. The results demonstrate that 10 μg/ml SLO had a toxic effect on cells at 24 h and 72 h (Fig. 1A and B). Therefore, non-cytotoxic SLO concentrations <10 μg/ml were used in subsequent experiments (0.25, 0.5, 1 and 2.5 μg/ml).

SLO inhibits RANKL-induced osteoclast differentiation in vitro. To evaluate the effect of SLO on osteoclast differentiation, TRAP staining was used to evaluate osteoclast differentiation. The RANKL-treated group exhibited more TRAP-positive multinucleated osteoclasts than the vehicle control group (Fig. 2A). SLO decreased the number of osteoclasts in a dose-dependent manner compared with the RANKL-treated group (Fig. 2B). This indicates that SLO inhibited osteoclast differentiation.

SLO inhibits RANKL-induced osteoclast fusion and bone resorption. To evaluate the effect of SLO on osteoclast fusion, focal adhesion staining was used to observe the cytoskeleton
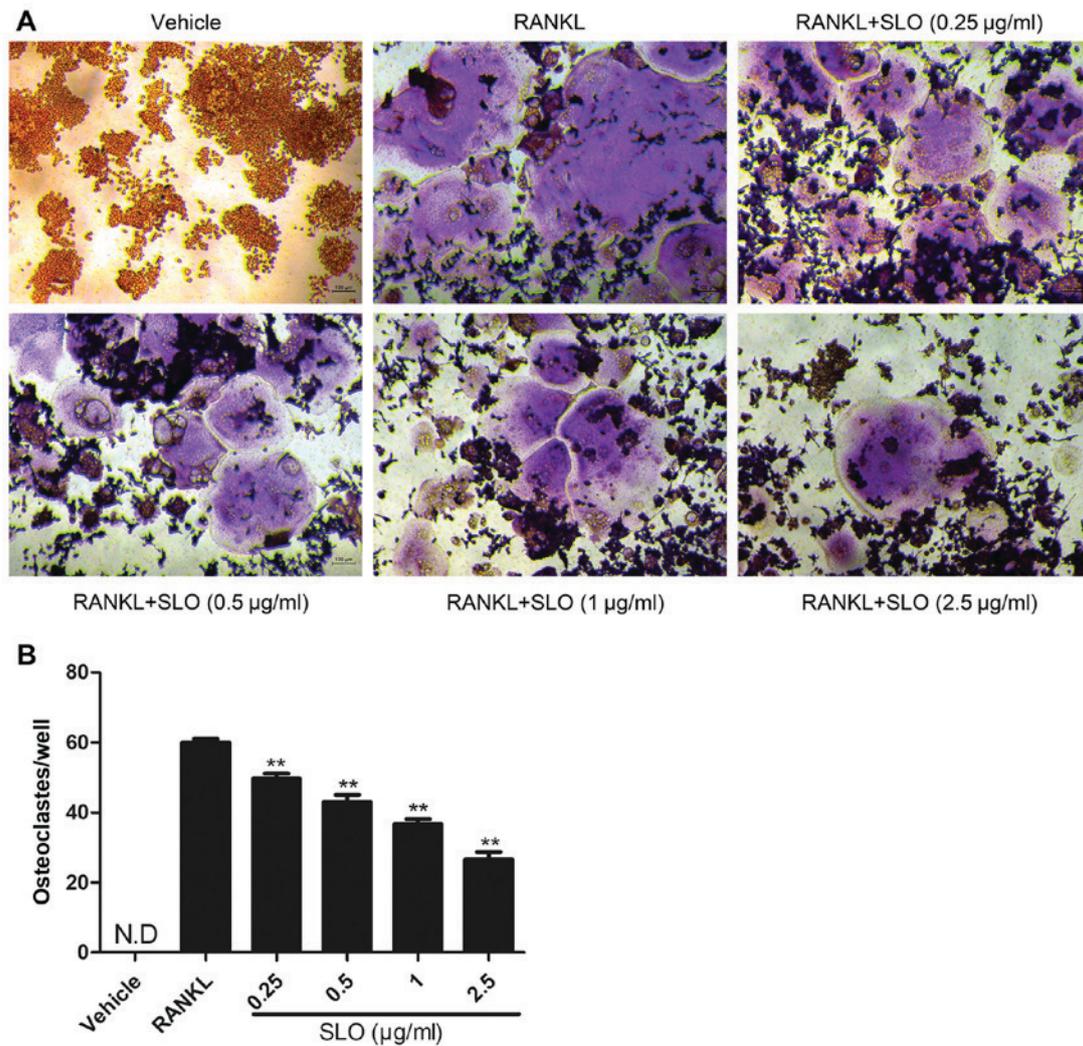
Figure 2. SLO inhibits osteoclast differentiation. (A) Raw 264.7 cells were stimulated by different concentrations of SLO and 50 ng/ml M-CSF and 50 ng/ml RANKL for 3 days. Cells were then fixed and stained for TRAP (magnification, x40). TRAP-positive cells with ≥3 nuclei were considered to be osteoclasts. (B) Quantification of osteoclast number in each well. The date in the figures represents the mean ± standard deviation. **P<0.01 vs. RANKL group. TRAP, tartrate-resistant acid phosphatase; RANKL, receptor activator of NF-κB ligand; SLO, streptolysin O; N.D., no data (no TRAP-positive cells detected).

and average nuclei. Prior to focal adhesion staining, Raw 264.7 cells were incubated with different concentrations of SLO for 3 days. Consistent with the TRAP results, SLO decreased the size of the multinucleated osteoclasts. The average number of nuclei in multinucleated osteoclasts was decreased in the SLO-treated groups compared with RANKL treatment, particularly in the 2.5 μg/ml SLO group (Fig. 3A and B). This indicates that SLO inhibited osteoclast fusion *in vitro*.

To further examine the effect of SLO on osteoclast resorption, Raw 264.7 cells were seeded into Osteo assay surface 96-well plates, and treated with RANKL and different concentrations of SLO for 5 days. The absorbed area of SLO-treated mature osteoclasts was significantly decreased compared with RANKL treatment (Fig. 3C and D). The result indicated that SLO reduced osteoclast bone resorption activity.

SLO inhibits RANKL-induced gene expression. The effect of SLO on the expression levels of a number of specific genes, including TRAP, CTR, integrinβ3, ATP6v0d2, DC-STAMP and MMP9, which were upregulated during osteoclast differentiation, were analyzed by RT-qPCR. The expression of

these genes was reduced in the SLO-treated groups compared with RANKL treatment, particularly in the 2.5 μg/ml SLO group. The result indicated that SLO inhibited osteoclastogenesis, which is consistent with the observed reduction in osteoclast differentiation and bone resorption (Fig. 4).

SLO inhibits RANKL-induced osteoclastogenesis by down-regulating c-FOS and NFATc1 via nuclear factor-κB (NF-κB). To analyze the signaling pathway underlying the effect of SLO on osteoclast differentiation, the expression of IκBα, p-IκBα, p65 and p-p6 were detected by western blotting. The cells were treated with or without 2.5 μg/ml SLO for 0, 5, 15 and 30 min. RANKL induced phosphorylation of IκBα at 5 min after activation (Fig. 5A). However, SLO pretreatment significantly inhibited RANKL-induced IκBα phosphorylation in Raw 264.7 cells. In addition, p65 phosphorylation was a significantly reduced by SLO. The effects of SLO on RANKL-induced NFATc1 and c-FOS expression were also investigated at the protein level. NFATc1 and c-FOS protein expression levels increased when the cells were stimulated with RANKL. However, SLO attenuated this increase, suggesting
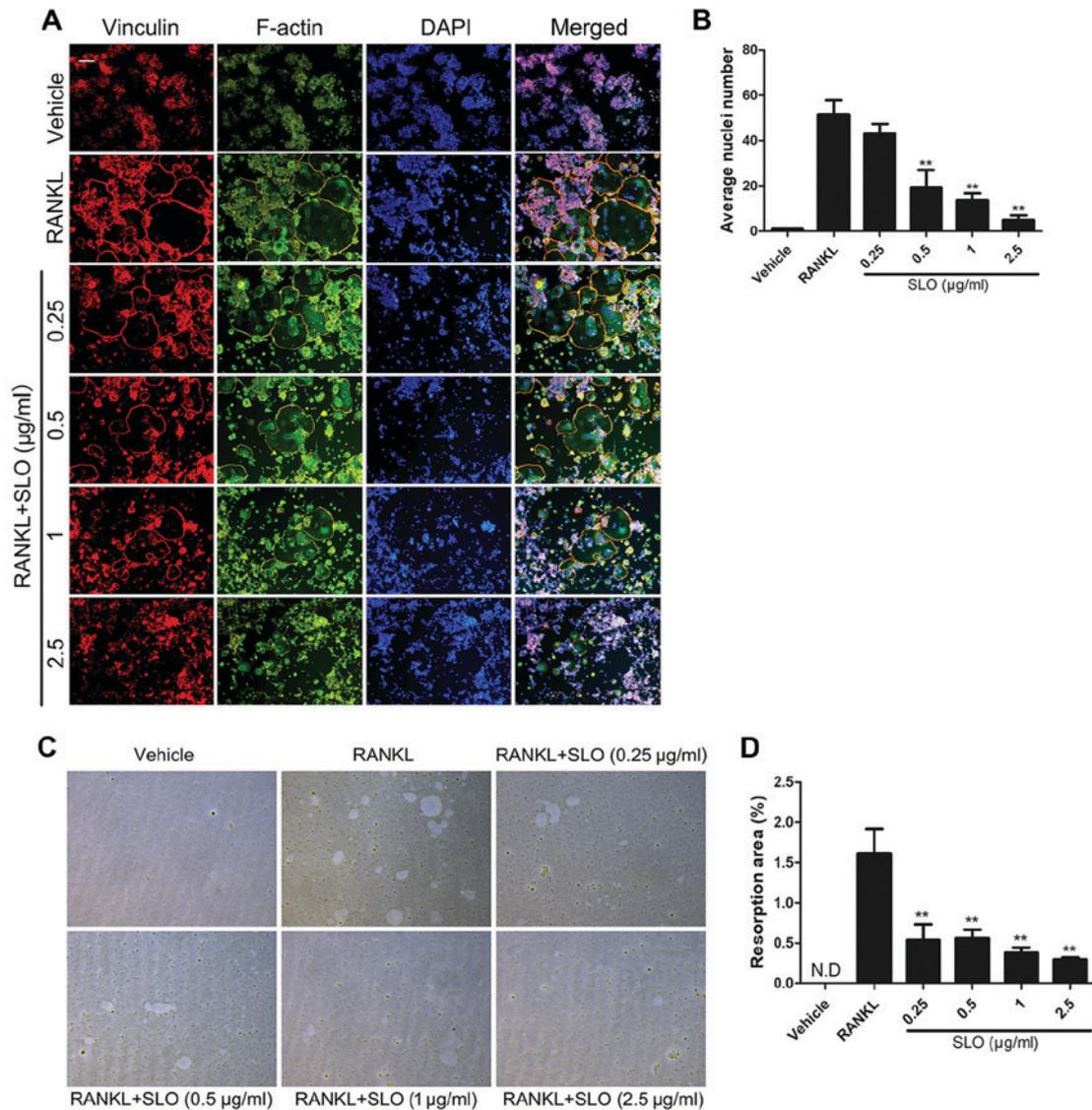
Figure 3. Osteoclast fusion and bone resorption assay. (A) Actin cytoskeleton and focal adhesion staining of RAW264.7 cells. F-actin was detected using TRITC-conjugated phalloidin (green). Vinculin was revealed using vinculin monoclonal antibody (red). Nuclei were revealed with DAPI (blue). Monochrome images of TRITC-conjugated phalloidin, vinculin monoclonal antibody vinculin and DAPI were merged (magnification, x40). (B) Average number of nuclei in each group (mean ± standard deviation of 3 fields of view). (C) Raw 264.7 cells were seeded into osteo assay surface 96-well plates and cultured in medium containing 50 ng/ml RANKL and 50 ng/ml M-CSF with different dosages of SLO for 5 days. Bone resorption area was observed under a light microscope (magnification, x40). (D) The area of resorption pits formed in the SLO-treated group was significantly lower than that of the control group (3 fields of view). **P<0.01 vs. RANKL group. TRITC, tetramethylrhodamine; RANKL, receptor activator of NF-κB ligand; SLO, streptolysin O; M-CSF, macrophage colony-stimulating factor; N.D., no data (no resorption pits detected).

that SLO suppressed RANKL-induced NFATc1 and SLO expression (Fig. 5B). Overall, this suggests that SLO inhibited RANKL-induced osteoclastogenesis via downregulation of the NF-κB/c-FOS/NFATc1 pathways.

SLO induces osteoclast apoptosis via the Bax/Bcl-2/caspase3 pathway. Flow cytometry was used to examine the apoptosis of osteoclasts treated with SLO. The proportion of cells in late apoptosis was increased in the SLO-treated groups compared with RANKL treatment (Fig. 6A and B). Bax/Bcl-2/caspase-3 is a classical pathway involved in apoptosis. The protein expression levels of Bax, Bcl-2 and caspase-3 were evaluated by immunoblotting. The results demonstrated that Bax and caspase-3 expression was increased in SLO-treated groups compared with the RANKL treatment, whereas Bcl-2 was

decreased (Fig. 6C). This indicated that SLO may induce osteoclast apoptosis via the Bax/Bcl-2/caspase-3 pathway.

Discussion

The Gram-positive bacterium, GAS, is a human pathogen, and ranked among the top 10 causes of infection-associated mortality worldwide (14). It can cause a wide spectrum of infections, ranging from self-limiting pharyngitis and impetigo, to invasive and life-threatening diseases, including streptococcal toxic shock syndrome and necrotizing fasciitis (15,16). There are ~700 million GAS infections and 1.8 million severe infections with a mortality rate >25% worldwide (14). Treatment failure occurs in 20-40% of patients treated with sensitive antibiotics (5); this creates an economic burden, particularly in
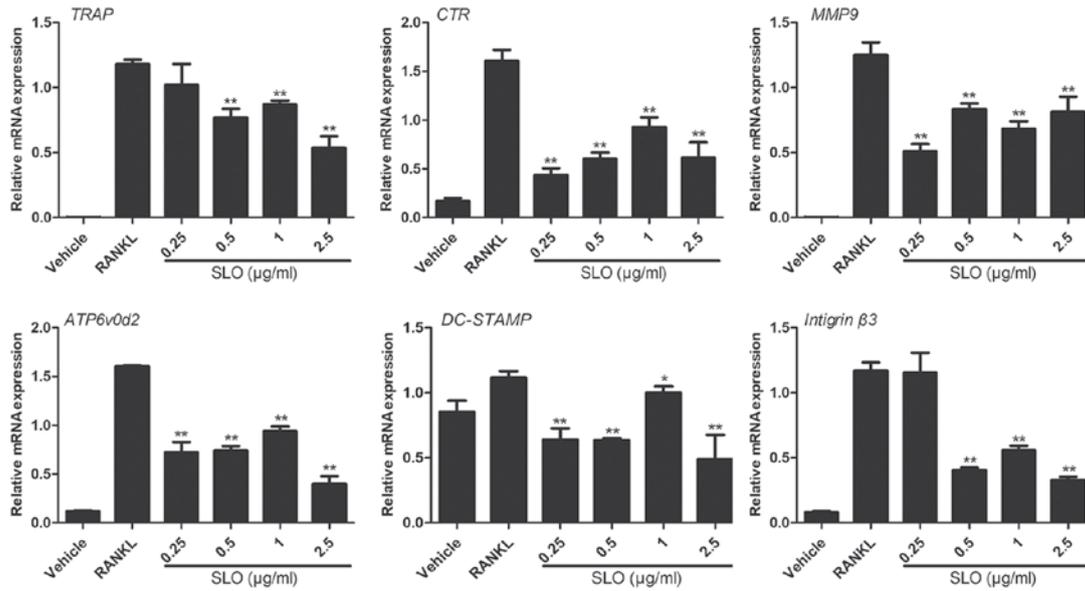
Figure 4. RT-qPCR analysis of mRNA during SLO stimulation. Raw 264.7 cells were cultured with M-CSF (50 ng/ml) and RANKL (50 ng/ml), with or without SLO. The expression of TRAP, CTR, MMP9, ATP6v0d2, DC-STAMP and integrinβ3 were analyzed by RT-qPCR. The results were normalized to the expression of GAPDH. The levels of these mRNAs were significantly reduced with SLO treatment (particularly 2.5 µg/ml SLO) compared to the control group. *P<0.05 and **P<0.01 vs. RANKL group. RT-qPCR, reverse transcription-quantitative polymerase chain reaction; RANKL, receptor activator of NF-κB ligand; M-CSF, macrophage colony-stimulating factor; SLO, streptolysin O; TRAP, tartrate-resistant acid phosphatase; CTR, calcitonin receptor; MMP9, matrix metalloproteinase-9; ATP6v0d2, ATPase H$^+$ transporting V0 subunit d2; DC-STAMP, dendritic cell-specific transmembrane protein.

developing countries. GAS is also one of the bacterial strains most responsible for bone infection, including septic arthritis and osteomyelitis (17), and accounts for ~15% of cases of nongonococcal bacterial arthritis (4). Biofilms may contribute to its infection efficacy (18). During septic arthritis and osteomy-elitis caused by GAS, abnormal activation of osteoclasts results in bone destruction (19-21). Osteoclasts are the only type of cells that have the function of bone resorption. However, there are few reports regarding the direct association between GAS and osteoclasts. To the best of our knowledge, the present study is the first to report that SLO, a typical product of GAS, suppresses osteoclast differentiation. *In vitro* studies demonstrated that osteoclast number, nuclei number and osteoclast resorption activity were significantly decreased by SLO, particularly in the 2.5 µg/ml SLO group. Consistent with these results, osteoclast differentiation marker genes, including TRAP, CTR, integrinβ3, ATP6v0d2, DC-STAMP and MMP9, were significantly decreased by SLO. It was further demonstrated that the NF-κB signaling pathway was involved in this process.

NF-κB signaling is one of the central pathways involved in differentiation and fusion of macrophage precursor cells (22). RANKL is a member of the tumor necrosis factor (TNF) family, and may act as a major regulator of bone loss. RANKL binding to the receptor activator of NF-κB (RANK) activates down-stream signaling pathways resulting in osteoclast formation (23). Following activation by RANKL, RANK-recruited TNF receptor associated factor 6 activates IκB kinase α, which promotes phos-phorylation and degradation of IκBα, resulting in the release of NF-κB (24). NF-κB dimers, containing p65 and c-Rel, are released into the cytosol via cascade reactions and translocated to the nucleus to enhance transcription of target genes, including c-FOS and NFATc1 (3,25). Thus, phosphorylation of IκBα and NF-κB (p65) are necessary for the activation of the NF-κB
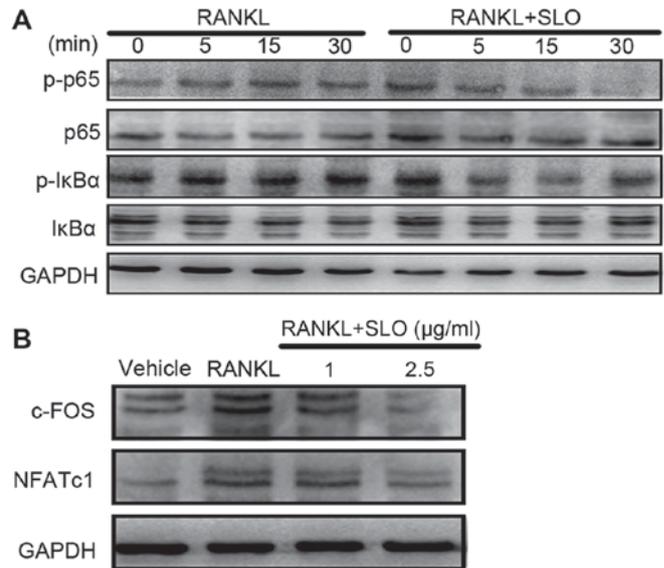

Figure 5. Western blot analysis of protein expression during SLO stimulation. (A) RAW 264.7 cells were stimulated with RANKL for the indicated dura-tions in the presence or absence of 2.5 µg/ml SLO. The effects of RANKL and RANKL + SLO are presented. (B) Raw 264.7 cells were treated with 1 and 2.5 µg/ml for 72 h. The protein expression of c-FOS and NFATc1 were signifi-cantly reduced in the experimental group. RANKL, receptor activator of NF-κB ligand; SLO, streptolysin O; p-, phospho-; IκBα, NF-κB inhibitor α; c-FOS, Fos proto-oncogene; NFATc1, nuclear factor of activated T cells cytoplasmic 1.

pathway. In the present study, SLO inhibited phosphorylation of IκBα and p65. c-FOS and NFATc1 are major transcription factors involved in osteoclastogenesis. Following activation by RANKL, the activator protein-1 transcription factor complex, which includes c-FOS, cooperates with NF-κB to induce NFATc1, has been reported to enable the transcription of osteoclast-specific
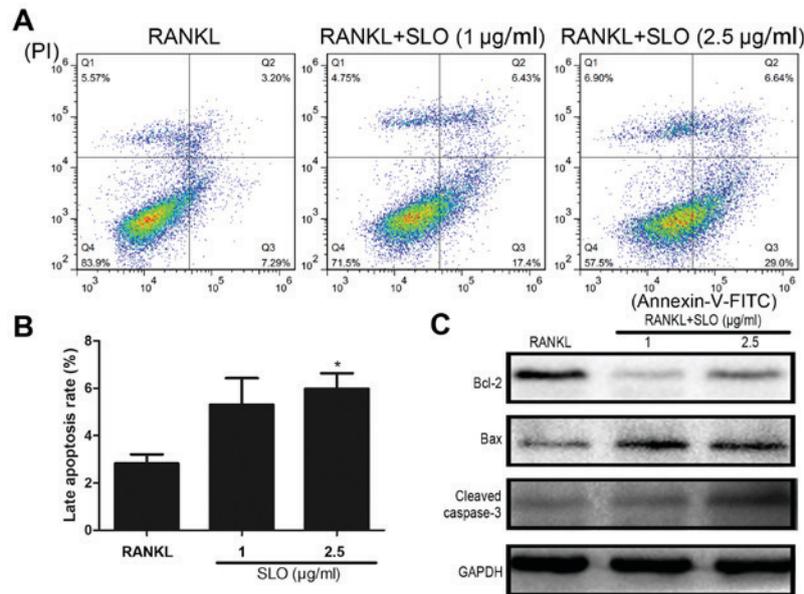
Figure 6. Osteoclast apoptosis assay. Raw 264.7 cells were cultured with 50 ng/ml M-CSF and 50 ng/ml RANKL with 1 or 2.5 μg/ml SLO for 72 h. (A and B) The cells then were stained with Annexin-V-FITC and PI fort 15 min in the dark for flow cytometry. *P<0.05 vs. RANKL group. (C) Western blotting was performed to analyze the protein expression of Bax, Bcl-2 and cleaved caspase-3. RANKL, receptor activator of NF-κB ligand; SLO, streptolysin O; PI, propidium iodide; FITC, fluorescein isothiocyanate; Bcl-2, BCL2 apoptosis regulator; Bax, BCL2 associated X apoptosis regulator.

genes (26). In the present study, SLO decreased the expression of c-FOS, and the translation of NFATc1, suggesting that SLO modulated the NF-κB/c-FOS/NFATc1 signaling pathway in RANKL-induced osteoclastogenesis. NFATc1 can regulate the expression of a number of genes associated with osteoclast differentiation and function. SLO inhibited the expression of osteoclastogenesis-associated marker genes, and decreased osteoclast number, the number of nuclei and osteoclast resorption activity. These results suggest that SLO exerted an inhibitory effect on RANKL-induced osteoclastogenesis via the NF-κB signaling pathway.

SLO can also trigger intracellular calcium concentration dysregulation during endoplasmic reticulum stress and mitochondrial depolarization, resulting in apoptosis of various cell types, including keratinocytes and macrophages (27,28). An increase in the Bax/Bcl-2 ratio can cause activation of caspase-3, which can induce apoptosis of mature osteoclasts (29). The protein expression pattern of Bax, Bcl-2 and cleaved caspase-3 was analyzed by western blotting in the current study. The protein expression of Bcl-2 was notably downregulated, while Bax and cleaved caspase-3 were upregulated by SLO. These results indicated that SLO induced apoptosis of mature osteoclasts. Apoptosis is involved in the mechanism of a number of agents which inhibit osteoclast bone resorption, including zoledronic acid (30). Through inducing osteoclast apoptosis, SLO may decrease the number of osteoclasts, and then reduce the area of resorption. It was also reported that an increased number of osteoclasts may be due to a decrease in apoptosis as a result of lower caspase-3 levels (31). The NF-κB pathway is closely associated with cell apoptosis and involved in the transcriptional regulation of various apoptosis-associated genes, including Bcl-2, Bax and caspase-3 (32-34). A previous study reported that inactivation or inhibition of NF-p65 may downregulate Bcl-2 family proteins, which in turn activates the caspase cascade, leading to apoptosis of C6 glioma cells (35).

In the present study, reduced NF-κB activation, upregulation of caspase-3 and upregulation of the Bax/Bcl-2 ratio were induced by SLO. According to these results, SLO may induce osteoclast apoptosis via the NF-κB-regulated apoptosis signaling pathway.

Notably, SLO inhibited RANKL-induced osteoclastogenesis, in accordance with a previous report in which it SLO monocyte-derived dendritic cell maturation (36). A previous study reported that GAS could promote expression of RANKL and induce bone loss during septic arthritis and osteomyelitis (19). It was also reported that SLO induced IL-6 and IL-8 by activating the NF-κB pathway in endothelial cells (37). During GAS infection, numerous inflammatory cells are recruited, resulting in secretion of TNF-α, IL-6 and IL-1β (20). These pro-inflammatory cytokines can also induce osteoclast differentiation and enhance bone resorption (38). GAS can produce other toxins, including peptidoglycan (PGN), M protein, streptolysin s and NADase, which can also interact with osteoclasts. For example, PGN from the gram-positive bacterium can induce osteoclast differentiation through a pathogen-associated molecular pattern pathway. SLO can also promote GAS survival and co-operate with other toxins, which may enhance GAS virulence. It may synchronize with NAD-glycohydrolase to prevent phagolysosome acidification and promote GAS survival in macrophages (12). Increased knowledge regarding the effects of other toxins on osteoclasts is required. A number of cell types of the bone, including osteoblasts and chondrocytes, protect against GAS infection, and all participate in the interaction between GAS and bone during bone infection *in vivo*. GAS can upregulate the expression of RANKL in osteoblasts (21). However, the present study only investigated SLO in the context of osteoclasts, and further research is required to extend the understanding of other cell types.

In conclusion, the present study demonstrated that SLO inhibited osteoclast formation and function by suppressing NF-κB signaling, and inducing mature osteoclast apoptosis.

The effect of SLO on RANKL-induced osteoclastogenesis may provide novel insight regarding regulation of the imbalance in the bone matrix caused by excessive osteoclast activity. The present study provides a foundation for treating bone loss due to GAS and other bacterial infections.

Acknowledgements

Not applicable.

Availability of data and materials

The datasets used and analyzed during the current study are available from the corresponding author on reasonable request.

Authors' contributions

JYi, RT and JF designed the experiments. JYi and YC performed the experiments. JYi, RT and JYa analyzed the data. JYi, RT and YC wrote the manuscript. JYi and YC revised the manuscript. All authors reviewed the manuscript.

Ethics approval and consent to participate

Not applicable.

Patient consent for publication

Not applicable.

Competing interests

The authors declare that they have no competing interests.

References

1. Harada S and Rodan GA: Control of osteoblast function and regulation of bone mass. Nature 423: 349-355, 2003.
2. Kim J, Yang J, Park OJ, Kang SS, Kim WS, Kurokawa K, Yun CH, Kim HH, Lee BL and Han SH: Lipoproteins are an important bacterial component responsible for bone destruction through the induction of osteoclast differentiation and activation. J Bone Miner Res 28: 2381-2391, 2013.
3. Moriarty TF, Schlegel U, Perren S and Richards RG: Infection in fracture fixation: Can we influence infection rates through implant design? J Mater Sci Mater Med 21: 1031-1035, 2010.
4. Schattner A and Vosti KL: Bacterial arthritis due to beta-hemolytic streptococci of serogroups A, B, C, F and G: Analysis of 23 cases and a review of the literature. Medicine (Baltimore) 77: 122-139, 1998.
5. Pichichero ME and Casey JR: Systematic review of factors contributing topenicillin treatment failure in *Streptococcus pyogenes* pharyngitis. Otolaryngol Head Neck Surg 137: 851-857, 2007.
6. Nilsson M, Sørensen OE, Mörgelin M, Weineisen M, Sjöbring U and Herwald H: Activation of human polymorphonuclear eutrophils by streptolysin O from *Streptococcus pyogenes* leads to the release of proinflammatory mediators. Thromb Haemost 95: 982-990, 2006.
7. Anderluh G and Lakey J: Proteins: Membrane binding and pore formation. Preface. Adv Exp Med Biol 677: v-vi, 2010.
8. Hotze EM, Wilson-Kubalek E, Farrand AJ, Bentsen L, Parker MW, Johnson AE and Tweten RK: Monomer-monomer interactions propagate structural transitions necessary for pore formation by the cholesterol-dependent cytolysins. J Biol Chem 287: 24534-24543, 2012.
9. Bhakdi S, Bayley H, Valeva A, Walev I, Walker B, Kehoe M and Palmer M: Staphylococcal alpha-toxin, streptolysin-O, and Escherichia coli hemolysin: Prototypes of pore-forming bacterial cytolysins. Arch Microbiol 165: 73-79, 1996.
10. Bricker AL, Carey VJ and Wessels MR: Role of NADase in virulence in experimental invasive group A streptococcal infection. Infect Immun 73: 6562-6566, 2005.
11. O'Seaghdha M and Wessels MR: Streptolysin O and its co-toxin NAD-glycohydrolase protect group A *Streptococcus* from Xenophagic killing. PLoS Pathog 9: e1003394, 2013.
12. Bastiat-Sempe B, Love JF, Lomayesva N and Wessels MR: Streptolysin O and NAD-glycohydrolase prevent phagolysosome acidification and promote group A *streptococcus* survival in macrophages. MBio 5: e01690-14, 2014.
13. Livak KJ and Schmittgen TD: Analysis of relative gene expression data using real-time quantitative PCR and the 2(-Delta Delta C(T)) method. Methods 25: 402-408, 2001.
14. Carapetis JR, Steer AC, Mulholland EK and Weber M: The global burden of group A streptococcal diseases. Lancet Infect Dis 5: 685-694, 2005.
15. Walker MJ, Barnett TC, McArthur JD, Cole JN, Gillen CM, Henningham A, Sriprakash KS, Sanderson-Smith ML and Nizet V: Disease manifestations and pathogenic mechanisms of group a *Streptococcus*. Clin Microbiol Rev 27: 264-301, 2014.
16. Good MF, Batzloff M and Pandey M: Strategies in the development of vaccines to prevent infections with group A *streptococcus*. Hum Vaccin Immunother 9: 2393-2397, 2013.
17. Pichichero ME: Group A beta-hemolytic streptococcal infections. Pediatr Rev 19: 291-302, 1998.
18. Freiberg JA, Mciver KS and Shirtliff ME: In vivo expression of *Streptococcus pyogenes* immunogenic proteins during tibial foreign body infection. Infect Immun 82: 3891-3899, 2014.
19. Sakurai A, Okahashi N, Nakagawa I, Kawabata S, Amano A, Ooshima T and Hamada S: *Streptococcus pyogenes* infection induces septic arthritis with increased production of the receptor activator of the NF-kappaB ligan. Infect Immun 71: 6019-6026, 2003.
20. Matsui H, Nakatani Y, Yoshida H, Takizawa A, Takeuchi O, Øverby A, Takahashi T, Murayama SY and Matsuo K: Flesh-eating *Streptococcus pyogenes* triggers the expression of receptor activator of nuclear factor-κB ligand. Cell Microbiol 18: 1390-1404, 2016.
21. Okahashi N, Sakurai A, Nakagawa I, Fujiwara T, Kawabata S, Amano A and Hamada S: Infection by *Streptococcus pyogenes* induces the receptor activator of NF-kappaB ligand expression in mouse osteoblastic cells. Infect Immun 71: 948-955, 2003.
22. Barnes PJ and Karin M: Nuclear factor-kappsBb: A pivotal transcription factor in chronic inflammatory diseases. N Engl J Med 336: 1066-1071, 1997.
23. Lacey DL, Timms E, Tan HL, Kelley MJ, Dunstan CR, Burgess T, Elliott R, Colombero A, Elliott G, Scully S, *et al*: Osteoprotegerin ligand is a cytokine that regulates osteoclast differentiation and activation. Cell 93: 165-176, 1998.
24. Ghosh S and Karin M: Missing pieces in the NF-kappaB puzzle. Cell 109 (Suppl): S81-S96, 2002.
25. Nepal M, Choi HJ, Choi BY, Yang MS, Chae JI, Li L and Soh Y: Hispidulin attenuates bone resorption and osteoclastogenesis via the RANKL-induced NF-kappaB and NFATc1 pathways. Eur J Pharmacol 715: 96-104, 2013.
26. Yamashita T, Yao Z, Li F, Zhang Q, Badell IR, Schwarz EM, Takeshita S, Wagner EF, Noda M, Matsuo K, *et al*: NF-kappaB p50 and p52 regulate receptor activator of NF-kappaB ligand (RANKL) and tumor necrosis factor-induced osteoclast precursor differentiation by activating c-Fos and NFATc1. J Biol Chem 282: 18245-18253, 2007.
27. Cywes Bentley C, Hakansson A, Christianson J and Wessels MR: Extracellular group A *Streptococcus* induces keratinocyte apoptosis by dysregulating calcium signaling. Cell Microbiol 7: 945-955, 2005.

28. Timmer AM, Timmer JC, Pence MA, Hsu LC, Ghochani M, Frey TG, Karin M, Salvesen GS and Nizet V: Streptolysin O promotes group A *Streptococcus* immune evasion by accelerated macrophage apoptosis. J Biol Chem 284: 862-871, 2009.
29. Scorrano L and Korsmeyer SJ: Mechanisms of cytochrome c release by proapoptotic Bcl-2 family members. Biochem Biophys Res Commun 304: 437-444, 2003.
30. Tai TW, Chen CY, Su FC, Tu YK, Tsai TT, Lin CF and Jou IM: Reactive oxygen species are required for zoledronic acid-induced apoptosis in osteoclast precursors and mature osteoclast-like cells. Sci Rep 7: 44245, 2017.
31. Kinning E, McMillan M, Shepherd S, Helfrich M, Hof RV, Adams C, Read H, Wall DM and Ahmed SF: An unbalanced rearrangement of chromosomes 4: 20 is associated with childhood osteoporosis and reduced caspase-3 levels. J Pediatr Genet 5: 167-173, 2016.
32. Shan RF, Zhou YF, Peng AF and Jie ZG: Inhibition of Aurora-B suppresses HepG2 cell invasion and migration via the PI3K/Akt/NF-kB signaling pathway *in vitro*. Exp Ther Med 8: 1005-1009, 2014.
33. Nehra R, Riggins RB, Shajahan AN, Zwart A, Crawford AC and Clarke R: BCL2 and CASP8 regulation by NF-kappaB differentially affect mitochondrial function and cell fate in antiestrogen-sensitive and-resistant breast cancer cells. FASEB J 24: 2040-2055, 2010.
34. Henrotin Y, Clutterbuck AL, Allaway D, Lodwig EM, Harris P, Mathy-Hartert M, Shakibaei M and Mobasheri A: Biological actions of curcumin on articular chondrocytes. Osteoarthritis Cartilage 18: 141-149, 2010.
35. Kiekow CJ, Figueiró F, Dietrich F, Vechia LD, Pires EN, Jandrey EH, Gnoatto SC, Salbego CG, Battastini AM and Gosmann G: Quercetin derivative induces cell death in glioma cells by modulating NF-κB nuclear translocation and Caspase-3 activation. Eur J Pharm Sci 84: 116-122, 2016.
36. Cortés G and Wessels MR: Inhibition of dendritic cell maturation by group A *Streptococcus*. J Infect Dis 200: 1152-1161, 2009.
37. Walev I, Hombach M, Bobkiewicz W, Fenske D, Bhakdi S and Husmann M: Resealing of large transmembrane pores produced by streptolysin O in nucleated cells is accompanied by NF-kappaB activation and downstream events. FASEB J 16: 237-239, 2002.
38. Lorenzo J: Interactions between immune and bone cells: New insights with many remaining questions. J Clin Invest 106: 749-752, 2000.